

LETTER TO THE EDITOR

Intercellular communications and metabolic reprogramming as new predictive markers for immunotherapy responses in gastric cancer

Dear Editor,

Immune-directed therapeutic approaches have changed the paradigm of cancer treatment. The tumor-immune microenvironment [1] is a dynamic milieu consisting of heterogeneous metabolic conditions such as low oxygen, nutrient deficiency, acidity, and interactions between multiple cell types. In particular, immune cells in the tumor microenvironment are vulnerable to cellular dysfunctions (because of metabolic reprogramming [2]) and engage in intercellular communications with neighboring cells, thereby contributing to a tolerogenic and incompetent immune environment. Here, we evaluated 84 metabolic pathways in 12,422 single cells from patients with gastric cancer (GC) [3] and predicted immune checkpoint blockade (ICB) responses associated with cell type-specific metabolic features using clinical outcome data from 45 GC patients treated with ICB at the Samsung Medical Center (the SMC cohort) (Supplementary Table S1) [4] and molecular subtype data from 497 GC patients treated at Yonsei Severance Hospital (the Yonsei cohort) (Supplementary Table S2) [5].

We first analyzed differences in the metabolic pathways in bulk GC samples between ICB responders and non-responders. The clinical data of the SMC cohort was subjected to systematic bioinformatics analyses for seven metabolic signatures [6]. In the responder group, biosynthetic pathways associated with amino acid synthesis ($P = 0.026$) and nucleotide synthesis ($P = 0.006$) were significantly enriched (Figure 1A). Differences in 84 metabolic pathways were also examined (Supplementary Figure S1A). The responder and non-responder groups demonstrated significant differences in 10 metabolic path-

ways. The highest differences were found in glutathione, glycerolipid, and nitrogen metabolic pathways (Figure 1B).

Furthermore, we predicted the responders and non-responders in the Yonsei cohort by analyzing the bulk transcriptome data using Tumor Immune Dysfunction and Exclusion (TIDE) for five molecular subtypes (Supplementary Table S3) [5, 7]. The stem-like subtype, which was associated with the worst prognosis [5], predicted the lowest proportion of responders (Figure 1C). Non-responders showed higher tumor immune dysfunction ($P = 0.014$) and exclusion scores ($P < 0.001$) than those shown by responders (Supplementary Figure S1B). Five metabolic pathways (thiamine metabolism, ether lipid metabolism, fatty acid elongation, phosphonate phosphinate, and cysteine methionine metabolism) were associated with the stem-like subtype (Supplementary Figure S1C). Further, in the non-responder group with the inflammatory and mixed-stroma subtypes, the glycosaminoglycan biosynthesis - chondroitin sulfate/dermatan sulfate pathway was significantly enriched (Supplementary Figure S1D).

Tumor-induced immune suppression can be ascribed to direct tumor factors and bystander tumor-related factors. To identify predictive biomarkers related to ICB responsiveness in terms of metabolic activity, we predicted the responses to ICB for each cell type using single-cell data. First, we prepared 8 simulated primary tumor samples for each patient with gastric single-cell data and predicted the ICB responses using TIDE. These samples were classified as 6 non-responder and 2 responder samples (Figure 1D; Supplementary Tables S5-S6). A total of 12,422 single cells were classified into 8 cell types, and each cell type showed a different response frequency (Figure 1E-1F). In the responder group, T and B cells related to innate immunity showed high metabolic activity. Macrophages had lower tricarboxylic acid cycle (TCA) levels in the responder group (false discovery rate [FDR] < 0.001 ; Figure 1G). The amino acid, carbohydrate, lipid, nucleotide, and TCA levels in adenocarcinoma cells were significantly higher

Abbreviations: KEGG, Kyoto Encyclopedia of Genes and Genomes; ICB, Immune-checkpoint blockade; SMC, Samsung Medical Center; TIDE, Tumor Immune Dysfunction and Exclusion; TCGA, The Cancer Genome Atlas

This is an open access article under the terms of the [Creative Commons Attribution-NonCommercial-NoDerivs](https://creativecommons.org/licenses/by-nc-nd/4.0/) License, which permits use and distribution in any medium, provided the original work is properly cited, the use is non-commercial and no modifications or adaptations are made.

© 2022 The Authors. *Cancer Communications* published by John Wiley & Sons Australia, Ltd. on behalf of Sun Yat-sen University Cancer Center

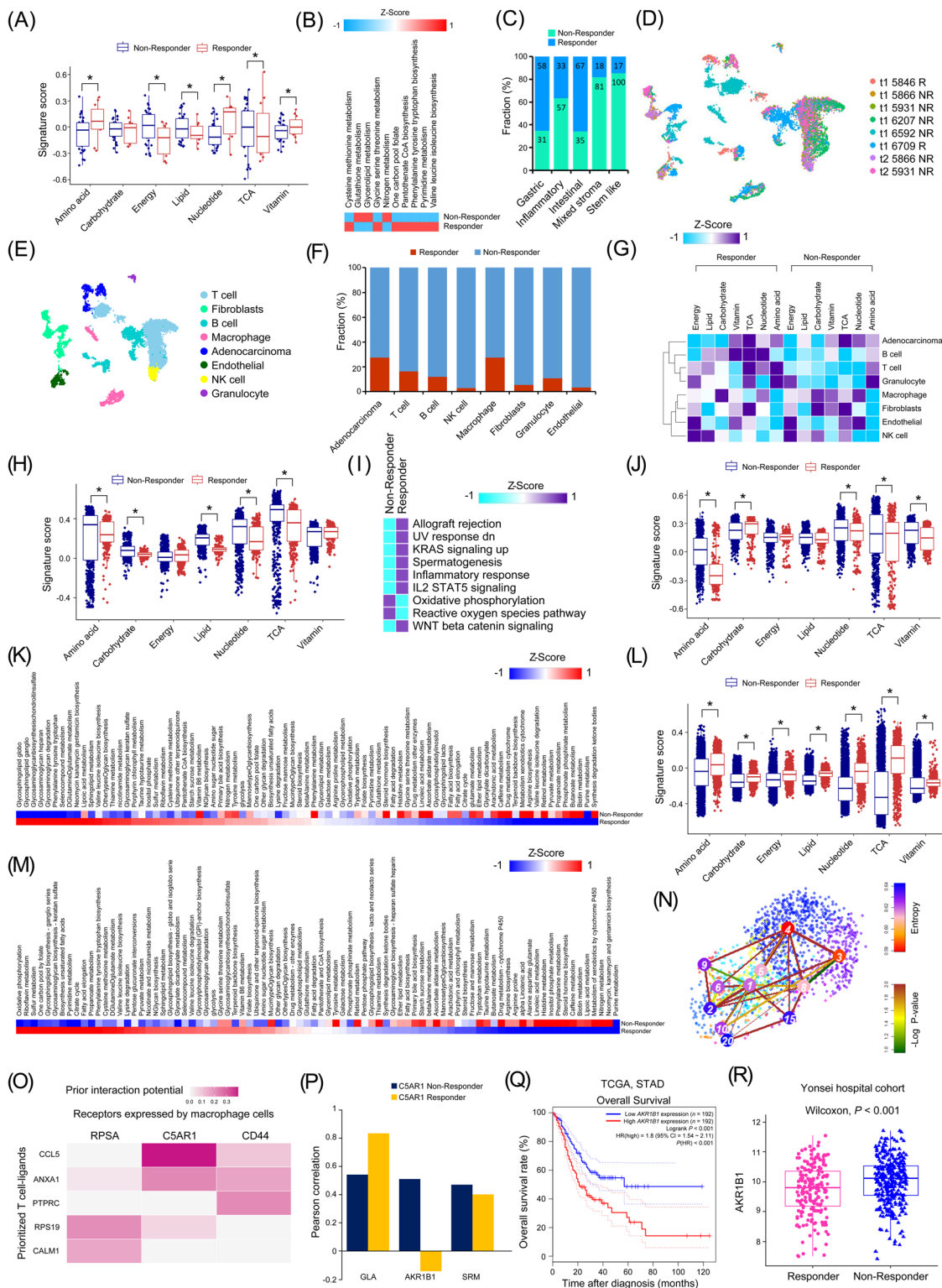


FIGURE 1 Intercellular communications and metabolic reprogramming as new predictive markers for immunotherapy responses in gastric cancer. (A) Boxplot of seven metabolic signatures related to immunotherapeutic responses in responders and non-responders in the SMC cohort ($n = 45$). (B) Metabolic pathways that differed significantly between responders and non-responders in the SMC dataset, among the 84 metabolic pathways studied. (C) Fractions of predicted responders and non-responders according to the molecular subtypes in the Yonsei cohort ($n = 497$). (D) UMAP plot of patient identification numbers from the gastric tumor dataset. (E) UMAP plot of 8 cell types for 8 samples from the gastric tumor dataset. (F) Bar graph showing fractions of predicted responders and non-responders in the gastric tumor dataset according to the 8 cell types. (G) Heat map of the activities of seven metabolic signatures between cells from responder and non-responder samples. (H) Boxplot of seven metabolic signatures related to immunotherapeutic responses using scRNA-seq data of

in responder samples than in non-responder samples (all $P < 0.001$; Figure 1H). Among other cancer hallmarks, allograft rejection, decreased responses to ultraviolet light, and increased KRAS signaling were significantly enriched in adenocarcinoma cells from responder samples (FDR < 0.001 ; Figure 1I). Specifically, adenocarcinoma cells from responder samples were highly enriched (FDR < 0.001) for the mucin-type O-glycan biosynthesis, glycosaminoglycan biosynthesis - keratan sulfate, nitrogen metabolism, valine, leucine, and isoleucine biosynthesis, and glycosaminoglycan biosynthesis - chondroitin sulfate/dermatan sulfate pathways (Supplementary Figures S2 and S3A).

Macrophages were predicted to be the most responsive cells at the single-cell level (Figure 1F). However, it is unknown how macrophages regulate responsiveness to ICB. Furthermore, M2 macrophages from responder and non-responder patients in the SMC and Yonsei cohorts showed no significant difference in terms of glycolysis (Supplementary Figures S1D & S2). Macrophages from responder patients showed low levels of amino acid ($P < 0.001$), nucleotide ($P = 0.003$), and vitamin ($P = 0.001$), but high levels of carbohydrate ($P = 0.002$) and TCA ($P = 0.009$) (FDR < 0.001 ; Figure 1J). Single-cell data revealed high glycan metabolic reprogramming in macrophages from responder patients (Figure 1K). The metabolic pathways in cells from responder and non-responder patients differed by 83.33%. In cells from responder patients, the glycosphingolipid biosynthesis - globo and isoglobo series, glycosphingolipid biosynthesis - ganglio series, and glycosaminoglycan biosynthesis - chondroitin sulfate/dermatan sulfate reference pathways were highly enriched.

Further analysis revealed enrichment of all the seven metabolic signatures in T cells from responder patients ($P < 0.001$; Figure 1L). Particularly, pyrimidine metabolism, propanoate metabolism, and the biosynthesis of unsaturated fatty acids were highly enriched (FDR < 0.001 ; Figure 1M). Clustering T cells according to the degree

of stemness using the VarID and StemID algorithms [8] showed that cluster 2 had the highest stemness whereas cluster 3 had the lowest stemness among others (Figure 1N, Supplementary Figure S3B). Of the cells constituting clusters 2 and 3, most (99%) of the T cells with the lowest stemness were in the non-responder group, and cluster 2 showed the highest stemness with over 90% in the responder group (Figure 1N). These results demonstrated that the immune response was activated while undergoing metabolic reprogramming (Supplementary Figure S3C) during T cell differentiation and activation.

As a cognate receptor interacting with C-C motif chemokine ligand 5 (CCL5), a prioritized T cell ligand, C5AR1, was predicted to be the most probable macrophage receptor (Figure 1O). C5a mediates macrophage polarization, and the combined inhibition of C5A/C5AR1 and programmed cell death 1 (PD-1) signaling have been predicted to show a synergistic anti-tumor effect [9]. The Pearson correlation analysis between C5AR1 and genes related to the glycerolipid metabolism pathways in the SMC dataset revealed an inverse correlation of the Aldo-Keto Reductase Family 1 Member B (AKR1B1) expression between the responder and non-responder groups (Figure 1P; Supplementary Table S7). AKR1B1 links glucose metabolism to epithelial-to-mesenchymal transition and is a potential cancer diagnostic marker [10]. We demonstrated that high AKR1B1 expression was associated with a poor prognosis, and it was expressed at significantly higher levels in the non-responder group (Figure 1Q-1R).

In this study, we unraveled how different immune cells engage in immunotherapy responses by cell type-dependent metabolic reprogramming at the single-cell level in GC. Our results demonstrated that intercellular conversation between macrophages and T cells in the non-responder group created a tumor metabolic microenvironment that suppressed overall immunity. Moreover, signal transduction in T cells and macrophages may affect glycerolipid metabolic reprogramming and be associated with

adenocarcinoma cells from responder and non-responder samples. (I) Heat map of the top-ranked cancer hallmark signatures among 50 cancer hallmark pathways in adenocarcinoma cells from responder and non-responder samples. (J) Seven metabolic signatures between macrophages from responders and non-responders using scRNA-seq data. (K) Heat map of 84 metabolic pathways in macrophages from responder and non-responder samples. (L) Boxplot of the seven metabolic signatures between T cells from responders and non-responders using scRNA-seq data. (M) Heat map of 84 metabolic pathways in T cells from responder and non-responder samples. (N) tSNE plot of stem-like T cell trajectories using VarID and StemID (blue: high entropy; red: low entropy). Cluster 2 has the highest entropy, and cluster 3 has the lowest entropy. Since the entropy shows the direction from high to low, the metabolic pathway activity on the left is significantly different between the two clusters. Oxidative phosphorylation, one carbon pool by folate, and sulfur metabolism are also significantly different between cluster 2 and cluster 3. (O) Heat map of prior interaction potential between prioritized T cell ligands and receptors expressed by macrophages. (P) Bar plot of Pearson correlation between C5AR1 and top three genes in the glycerolipid, glutathione, and nitrogen metabolic pathways in responders and non-responders from the SMC cohort. (Q) Kaplan-Meier overall survival curves of the patients with high and low expression of AKR1B1 in TCGA STAD dataset. (R) Boxplot of AKR1B1 expression in responders and non-responders from the Yonsei cohort ($P < 0.001$). Abbreviations: SMC, Samsung Medical Center; TCA, tricarboxylic acid cycle; UMAP, Uniform manifold approximation and projection; scRNA-seq, single-cell RNA-sequencing; tSNE, t-distributed stochastic neighbor embedding; TCGA, The Cancer Genome Atlas

immunotherapeutic outcomes in non-responder patients. We speculate that lipid components of the cell membrane might affect the phagocytosis of macrophages that would explain the reprogrammed glycerolipid metabolic activity in non-responders. Collectively, this study provides substantial metabolic insights for developing precision immunotherapy, which may help achieve better immunotherapeutic outcomes and potentially overcome ICB resistance in GC patients.

DECLARATIONS

ETHICS APPROVAL AND CONSENT TO PARTICIPATE

Not applicable

PATIENT CONSENT FOR PUBLICATION

Not applicable

AVAILABILITY OF DATA AND MATERIAL

All data are available in the main text and supplementary materials.

COMPETING INTERESTS

Authors declare that they have no competing interests.

FUNDING

This research was supported by a grant from the National Research Foundation, funded by the Ministry of Science and Information & Communication Technology, Republic of Korea (2018R1A5A2025079).

AUTHORS' CONTRIBUTIONS

Conceptualization: JYS, JHC; Methodology: JYS, JHC; Data analysis: JYS; Writing – original draft: JYS; Writing – review & editing: JYS, JHC; Supervision: JHC; Project administration: JHC; Funding acquisition: JHC; Formal analysis: JYS; Both authors contributed to the interpretation of the results. Both authors have read and agreed to the published version of the manuscript.

Ji-Yong Sung¹ 
Jae-Ho Cheong^{2,3,4}

¹Department of Laboratory Medicine, Yonsei University College of Medicine, Seoul 03722, Korea

²Department of Surgery, Yonsei University College of Medicine, Seoul 03722, Korea

³Yonsei Biomedical Research Institute, Yonsei University College of Medicine, Seoul 03722, Korea

⁴Department of Biochemistry & Molecular Biology, Yonsei University College of Medicine, Seoul 03722, Korea

Correspondence

Jae-Ho Cheong, Department of Surgery, Yonsei University College of Medicine, Seoul 03722, Korea.

Email: jhcheong@yuhs.ac

ORCID

Ji-Yong Sung  <https://orcid.org/0000-0002-8397-1691>

REFERENCES

1. Vander Heiden MG, DeBerardinis RJ. Understanding the Intersections between Metabolism and Cancer Biology. *Cell*. 2017;168(4):657-669.
2. Coleman MF, Cozzo AJ, Pfeil AJ, Etigunta SK, Hursting SD. Cell Intrinsic and Systemic Metabolism in Tumor Immunity and Immunotherapy. *Cancers (Basel)*. 2020;12(4).
3. Sathe A, Grimes SM, Lau BT, Chen J, Suarez C, Huang RJ, et al. Single-Cell Genomic Characterization Reveals the Cellular Reprogramming of the Gastric Tumor Microenvironment. *Clin Cancer Res*. 2020;26(11):2640-2653.
4. Kim ST, Cristescu R, Bass AJ, Kim KM, Odegaard JI, Kim K, et al. Comprehensive molecular characterization of clinical responses to PD-1 inhibition in metastatic gastric cancer. *Nat Med*. 2018;24(9):1449-1458.
5. Cheong JH, Yang HK, Kim H, Kim WH, Kim YW, Kook MC, et al. Predictive test for chemotherapy response in resectable gastric cancer: a multi-cohort, retrospective analysis. *Lancet Oncol*. 2018;19(5):629-638.
6. Peng X, Chen Z, Farshidfar F, Xu X, Lorenzi PL, Wang Y, et al. Molecular Characterization and Clinical Relevance of Metabolic Expression Subtypes in Human Cancers. *Cell Rep*. 2018;23(1):255-269 e4.
7. Jiang P, Gu S, Pan D, Fu J, Sahu A, Hu X, et al. Signatures of T cell dysfunction and exclusion predict cancer immunotherapy response. *Nat Med*. 2018;24(10):1550-1558.
8. Grun D, Revealing dynamics of gene expression variability in cell state space. *Nat Methods*. 2020;17(1):45-49.
9. Ajona D, Ortiz-Espinosa S, Moreno H, Lozano T, Pajares MJ, Agorreta J, et al. A Combined PD-1/C5a Blockade Synergistically Protects against Lung Cancer Growth and Metastasis. *Cancer Discov*. 2017;7(7):694-703.
10. Wu X, Li X, Fu Q, Cao Q, Chen X, Wang M, et al. AKR1B1 promotes basal-like breast cancer progression by a positive feedback loop that activates the EMT program. *J Exp Med*. 2017;214(4):1065-1079.

SUPPORTING INFORMATION

Additional supporting information may be found in the online version of the article at the publisher's website.